COEXISTENCE OF FLOW REGIME TRANSITIONS IN FOAMING TRICKLE BED REACTOR

Vijay Sodhi

Department of Chemical Engineering, Beant College of Engineering and Technology, Gurdaspur, Punjab, India, E-mail: vijaysodhi10@gmail.com

Abstract

The myth of coexistence of flow regimes in trickle bed reactor were experimentally explored using 40 ppm and 60 ppm highly foaming aqueous surfactant-air system. Since the last publication, none of literature present adequate experimental investigation of these flow irregularities arise near regime transitional boundary. The influence of physiochemical as well as hydrodynamic variables has been investigated to verify the possibilities of coexistence of flow regimes at corresponding liquid and gas flow velocities. The increment in the gas-liquid throughput resulted in an uneven disturbance velocity leads to formation of coexistence of flow regimes. The implementation of modified liquid-gas distributor slightly improve the flow maldistribution over packed bed but limited to low gas-liquid superficial velocities and temperatures. A relatively new technique, two gas-liquid distributors has been attempted first time to nullify the these kind of flow irregularities arise, trends evident an outstanding improvement of regime flow patterns compared with earlier cases.

Keywords: foaming flow; pulsing; hydrodynamics; flow maldistribution.

1. Introduction

Trickle flow is defined as gravity driven co-current flow of liquid-gas over a packed bed of catalyst particles. The hydrodynamic description of foaming trickle bed reactors is a complex field of study. The major complexity issue is the existence of multiple hydrodynamic flow patterns, also referred to as hydrodynamic regimes. A number of trickle to pulse flow regime (shown in Figure 1) studies have been done for small diameter columns. Under these conditions, the flow patterns limited by the diameter of the column and covers the whole cross section. Larger columns may not exhibit this but pulsing and trickling flow can coexist in the column [1]. The operation of the reactor is favorable in the pulse flow regime in which liquid/solid mass transfer coefficients are credibly higher than in the trickling flow [2]. The gas bubbles in form of pulses appears at high liquid flow rates and low gas flow rates. During this, the liquid is the continuous phase and the gas moves followed as dispersed bubbles leads to formation of the pulsing-foaming flow regime [3]. The significance of pulsing flow are well documented in literature. The studies of pulse flow characteristics at elevated pressures are very recent [4-6].
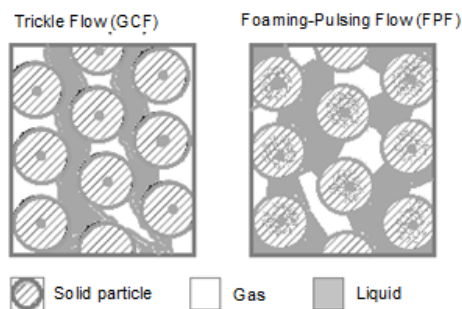

Figure 1. Schematic representation of trickle flow regime and foaming pulsing flow regime.

Since flow regimes persist in various industrial applications, it is important to unfold the multiplicity of flow patterns on basic characteristics occur during regime transition change [7]. On the basis of experimental evidences, many efforts have been done in order to establish theoretical criterion to correlate the regime boundaries and yield efficiency in a adequate way [8]. One of the ways to improve the efficiency of the TBRs operation was the idea of operation at periodically changing supply with liquid phase. It can be carried out using the method of temporary stoppage of the liquid flow through the reactor by the ON-OFF method [9]. To elaborate multiplicity of hydrodynamic regimes arise during the transition change in foaming systems, the dynamic liquid saturation in concurrent downflow column is more prominent criteria in this concerns. Most of the researches observed liquid holdup decreases with the increase in gas velocity like in the GCF and PF/FPF regime. However, the increase in mean liquid velocity causes in increase of dynamic liquid saturation value [11]. A number of researches proposed mathematical correlations for gas-liquid saturation in terms of Lockhart - Martinelli [10] using different bed configurations and packing characteristics. But these correlations did not considered the effect of flow behavior during coexistence of regimes. There is not even a single investigation (with experimental evidences) published concerned to this important issue.

A number of researchers proposed different regime flow map to correlate transitions between trickle and foaming-pulsing flow concerned to ambient temperature and pressure. In last decade, studies [9,12-14] of trickle bed hydrodynamics for foaming systems characterized the trickle-to-pulse flow regime transition for elevated pressure drop up to 2 MPa. Instead of this, none of literature reported dual nature of flow regimes with an experimental. The irregularities of regime flow or flow pattern exploits an uneven chemical reactions, abrupt input variables and further associated heat effects [15-16]. The increased system temperature results a rapid rise in pressure drop due to faster foam drainage and foam bubble collapse when the gas flow introduced to liquid feed [17-19]. Much about responsible reasons behind present issue remains to be discovered.

Many reactions involved in trickle bed operations are mass transfer limited. An increasing mass transfer driven with gas-liquid periodic flow interruption have explored pulsation wave switching of liquid flow velocity to a considerable level [20-21]. However, for the same amplitude of pulsing, variations were much less than those observed for flow interruption. Sodhi et al. [7] reported a significant increment in pulse velocity with gas-liquid flow rates. Their studies also explained the improvement of conversion yield through foaming flow variation is widely depends upon the surface tension of system to be analyzed. Burghardt et al. [4.13] introduced electrical conductivity probe techniques to evaluate flow variables (including velocity, pulse frequency and pulse length) for a number of gas–liquid systems. A number of researches found no influence of liquid/gas velocities on hydrodynamics of air-water systems [7,11,14].

Trickle-bed reactors poorly eliminate the heat involved in process reaction which further leads to hot spot formation. This criterion strongly depends on the type of flow regime as demonstrated by Boelhowver [22]. Earlier, Tsochatzidis et al. [1] reported, over a liquid flow rate of 0.015 m/s, nature of pulsing variables depends only on gas flow velocity. This statement could not be confirmed with the reactor installation used by Sodhi et al. [7] The transition from trickle to pulsing flow results a prominent increase in heat transfer rate [6,9]. It was also observed that for pulsing flow, the heat transfer rate were 3- times higher than that recorded in the trickle flow cycle [12]. The visual observation through wall of reactor were investigated for solid glass beads reported an increase in pulse frequency corresponds to gas-liquid flow velocities [8,14]. During regime transition change from trickle to pulse flow, the excess liquid transport is more responsible for concentration of pulses appeared at desired gas flow velocity. However, the key to excess liquid transport will be the bigger amount of pulses but depletion in dynamic liquid holdup.

Bartelmus et al. [9,12]. revealed the periodic liquid feeding were chosen in such a way so as to induce natural pulsations in the impulse of the liquid. Correlations enabling to calculate the values of the hydrodynamic parameters and liquid/solid mass transfer coefficients of the reactor operating in liquid induced pulsing flow regime. But unable to elaborate the coexistence of regimes. This phenomenon during transition change from PF to FPF remains unsaturated/ disturbed for whole passage of time. Where Tsochatzidis et al.[1] interpreted this as beginning of bubble/spray flow regime where in absence of any main pulse frequency. However, the catalyst bed cannot be liquid saturated at gas flow velocity beyond 0.37 m/s due to technical as well

as hydrodynamic difficulties. Here more noticeable thing, in non foaming systems this pheno-menon is absent at elevated temperatures too. Periodic flow variation experiments revealed that the reactor external forces can change the hydrodynamic regime from trickling to pulsing or foam-pulsing [23-24].

It is clear that coexistence of hydrodynamic regimes in the form of unstable pulsing-foaming could be significantly affected by physiochemical parameters of gas-liquid systems to be analyzed. However, needed a further study by a more detailed representation of foaming flow transport over catalyst particles. Preliminary observations reported that the maldistribution of pulsing-foaming over bed loading is abruptly decreased or increased with very small ranges of 0.010 $kg.m^{-2}s^{-1}$ and 0.255 $kg.m^{-2}s^{-1}$ in gas and liquid flow velocities respectively. This kind of instabilities are not reported in any literature. This surprising change is much responsible for dual natured flow during regime transitional change in present study foaming systems.

2. Experimental section

Literature studies show, trickle flow is more uniform for the particle diameter less than 6 mm [13,24]. A schematic of the experimental setup is shown in Figure 2. The experimental section mainly consists of a transparent glass column of 120 cm long, the movement of phases being allow concurrent down over the catalyst bed. The gas and liquid entry were provided from top of the column. Experiments were carried out on a 10 cm diameter glass column fed upto 100 cm height with spherical glass beads of size 7.12 mm. This dimension were chosen due to the fact that to achieve more uniform liquid distribution. Air coming from the compressor was first saturated with liquid in a saturator before introducing over catalyst bed. The liquid was pumped from a liquid feed tank through a rotameter (to measure the desired flow rate). For the even distribution of liquid, a distributor was provided at the top of the packed section. The solid catalyst packing was supported on a stainless steel mesh. The liquid was introduced into the column at the desired air flow rate. Air is drawn from compressor through pressure regulator. There are two kinds of distributors were used in present study. Distributor-A (Figure 3) is factory equipped and made in accordance to common industry standards of TBR. The dynamic liquid saturation and pressure drop related trends obtained by using similar dimensioned distributor has already been listed in [7,11,19].

Solenoid valve in the air flow is provided so as to cut the supply of air instantly for the measurement of dynamic liquid saturation, air and liquid phase after transverse the length of the packing were discharged at the bottom of the column through a conical separator/discharger. For each successive run flow rate was gradually increased to next desired. A mild foam was noticed in the column at small liquid and gas flow velocities. Manometer valve was also closed and air supply at 0.0312 $kg.m^{-2}s^{1}$ pressure was introduced. Now the setup was left in position for 30 min. The liquid flow was run for 20 min for complete wetting of the packing. Small quantity of air was now introduced into the column and slowly the airflow rate was brought to its desired rate within 2-3 min. Both the phases were allowed to flow downward over the packing for 20-25 min, which is necessary for the flow to attain a steady state. The flow pattern across the reactor column was visually observed. The liquid was collected in the column for 30-45 min till formation for stable PF/FPF at high flow rates.

The surfactant concentrations between 15-60 ppm SLS were high enough to investigate foaminess in TBR and to unfold the reactor hydrodynamics. This study involves alternating gas and liquid ON/OFF arrangements to yield gas/liquid flow variably. Experiments at variable temperatures and pressure were also carried out in reactor to visualize the foam structures to understand their behaviour during the cyclic operation. Formation of foam structures caused drastic increase in reactor pressure regardless of system temperature. While pressure drop is recorded with the help of electronic pressure transducers situated on the right to top of the column. Temperature were recorded from electronic transmitters situated on the two right ends of the column. The dynamic liquid saturation was studied by liquid drainage method. Since the packing to be used is non-porous, internal holdup is taken as zero.
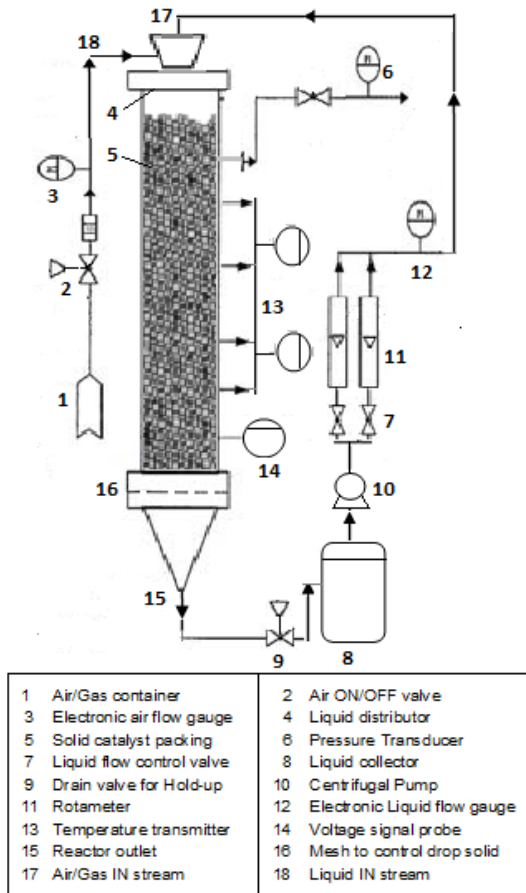
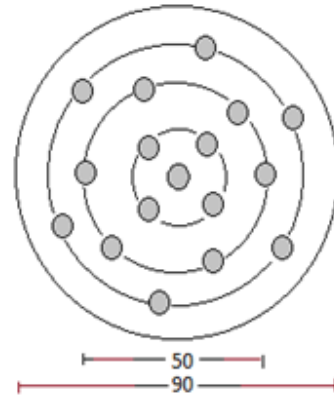Fig. 2. Experimental set-up used for present study

Fig. 3. Schematic of gas-liquid Distributor-A situated on the top of reactor column. Total number of holes: 17, diameter of each hole: 5mm

During FPF regime, upto 75% of the sectional area of the reactor witnessed an extensive foaming over catalyst bed surface. While using transparent glass column, regime transitional change observations were primarily made on visual inspections. It is observed that, GCF zones were more to the centred-front side of the catalyst bed column. But in FPF regimes, foaming-pulsing concentration observed were more in both central front and central-left side of the bed column. As literature trends show, it is impossible to work in the HIPF regime alone, in case of highly foamed liquids, the region in which induced pulsing flow occurs was practically the same as for the self-induced GCF/FPF. Therefore, measurements were done under cyclic mode. In present study, to verify the coexistence of regimes in foamed TBR, the influence of different hydrodynamics as well as physiochemical parameters on 40 ppm and 60 ppm sodium lauryl sulphate aqueous solution has been investigated at three different temperatures. The physiochemical description of investigated systems has been given in Table 1.

Table 1. The physiochemical description of corresponding parameters, liquid surface tension σ_L, density ρ_L, liquid viscosity μ_L, liquid diffusivity D_L observed for present study.

	Air-Water (non-foaming)			Air-40 ppm SLS system (severely foamed)			Air-60 ppm SLS system (severely foamed)		
T [°C]	18	28	60	18	28	60	18	28	60
σ_L [10^{-3} N m^{-1}]	70	69.8	67.1	47.9	47.2	45.2	44.9	44.5	41.4
ρ_L [kg m^{-3}]		997.8[a]			999.4[a]			999.9[a]	
μ_L [10^{-3} kg.m^{-1}s^{-1}]	1.00	1.01	1.01	1.17	1.16	1.10	1.19	1.19	1.15
D_L [10^{-9} m^{2}s^{-1}]	2.70[b]	2.70	2.66	1.91[b]	1.87	1.71	1.84[b]	1.80	1.66

[a] same at all temperatures; [b] Liquid diffusivity determined using correlation of Wilke and Chang [25]

3. Results and discussion

3.1. Effect of Foam Stability.

In order to observe effect of temperature on foam parameters like stability, drainage and breakdown, simple foam evaluation tests were performed at regular intervals. This generally follows foaming rise upto a certain height of bed and time elapsed for foam breakdown was recorded. Results witnessed the favorable temperature for longer foam stability is 28-40°C. Foam breakage observed is persists with passage of time (most rapidly in higher temperature of 60°C) during continuous cyclic operations therefore stability is more at room temperature but severe foam is observed at higher temperatures. The flow map with marked ranges of changes in velocity of gas-liquid phases in present study showed in Figure 4.

A few number of flow maps are available to predict the regime transition in foaming systems in TBR. Most reliable of these maps (eq 1) first proposed by Charpentier and Favier [30] On the basis of which, [26] and [31] produced a modified form of regime transition maps by considering influence of different catalyst sizes. The parameter λ and ψ express the physico-chemical properties of the gas-liquid system to be studied. Further in last decade, [8] and [12] done a outstanding experimentation to produce a more prominent form of regime boundary evaluation at corresponding low surface tension systems. For present study, Figure 5 shows the range of transition lines for coexistence of flow regimes at three different temperatures has been plot on the flow coordinates proposed by [30]. Figure 5 also gives comparison amongst present study over the GCF to PF/FPF transition boundaries proposed by different researchers. Here noticeable thing is, most of the flow points approves the present range of data in accordance to transition boundary proposed by [26] and [31].

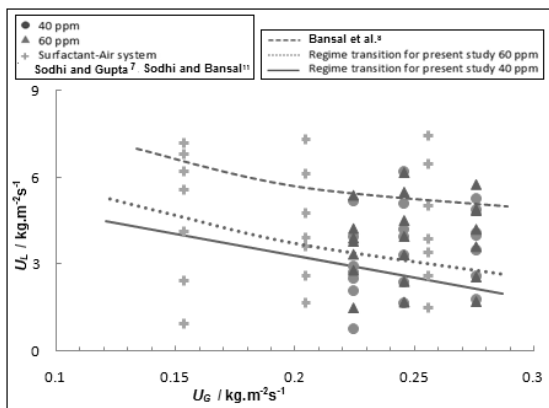$$\frac{L\Psi\lambda}{G} = \frac{G}{\lambda} \tag{1}$$

Fig. 4. Range of experimental gas and liquid flow velocities observed in present study of air-non-foaming water and air-foaming aqueous SLS systems. The dashed line, regime transition boundary for air-water system (T=28°C) obtained by Bansal *et al.* [8]
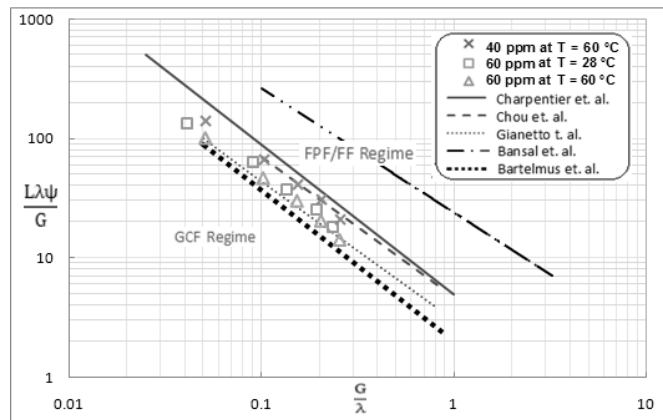

Fig. 5. Experimental points (symbols) for coexistence of flow regime transition plotted using regime flow coordinates proposed by Charpentier and Favier [30]

3.2 Dynamic Liquid Saturation (β_{exp})

It is observed that from Figure 6, at the highest temperature, the dynamic liquid holdup rapidly decreases with liquid flow rate for both 40 ppm and 60 ppm surfactant water-air system. As discussed, in foaming systems, regime transition change is repelled towards higher liquid flow while considerable gas flow available. The decrease of dynamic liquid holdup with increasingly gas flow at corresponding elevated temperatures confirming the persistence of this behaviour compared in published data. Measurements in smaller liquid flow portion of the pulse cycle show the reaction rate is about twice of the reaction concentration accumulate during trickle flow at same corresponding liquid flow velocities.
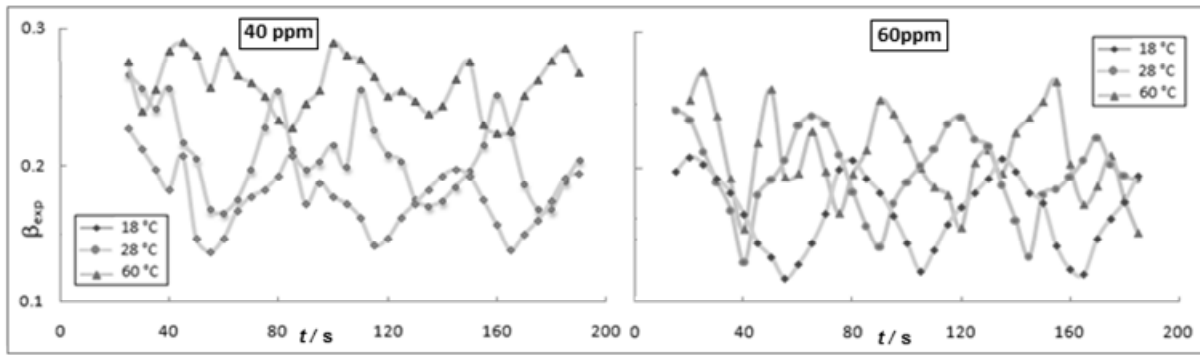
Fig. 6. Experimental dynamic liquid saturation(β_{exp}) as a function of time at corresponding temperature. For 40 ppm solution, U_G = 0.2429 kg.m^{-2}s^{-1} and U_L = 5.931-6.580 kg.m^{-2}s^{-1}. For 60 ppm solution, U_G = 0.2770 kg.m^{-2}s^{-1} and U_L = 3.808-4.210 kg.m^{-2}s^{-1}.

Experimental observations of both 40 ppm and 60 ppm surfactant water-air systems has been compared with literature data [7,11,27] in Figure 7. Present trends significantly shows the influence of elevated temperatures on dynamic liquid saturation decreases with increase in extensive foaming over bed (severe at 60°C) for both investigated systems. The zigzag trends verified the uneven nature of dynamic liquid saturation observed during dual natured flow for both systems. Here more noticeable thing is, this point is act as transition for coexistence of regimes but strongly not termed as regime transition line for GCF to FPF. Further with little change in gas or liquid flow velocities, this boundary leads to complete pulsing-foaming flow or regime transition to FPF.
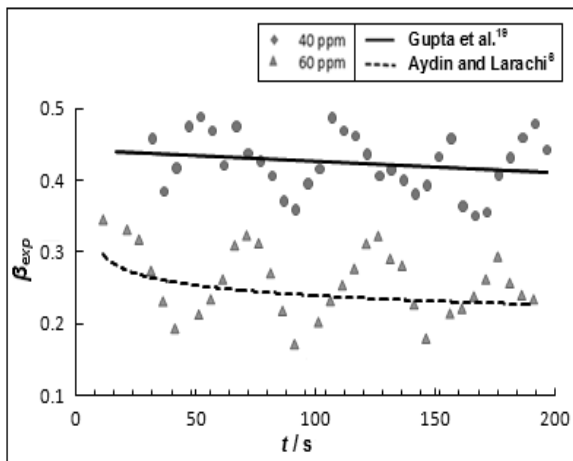

Fig. 7. Experimental dynamic liquid saturation (symbols) and those reported in literature (lines) as a function of time. Where for 40 ppm solution, T = 60°C, U_G = 0.2210 kg.m^{-2}s^{-1} and U_L = 6.239 kg.m^{-2}s^{-1}. Similarly, for 60 ppm solution, T = 60°C, U_G = 0.2210 kg.m^{-2}s^{-1} and U_L = 5.880 kg.m^{-2}s^{-1}
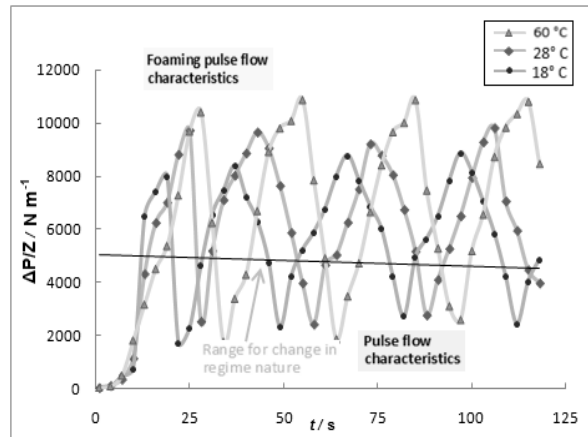
Fig. 8. Evidences of uneven two-phase pressure drop trends observed correspond to 60 ppm aqueous SLS, U_G = 0.2770 kg.m^{-2}s^{-1} and U_L = 3.808-4.210 kg.m^{-2}s^{-1} respectively

3.3. Change in Two-phase Pressure Drop

It is important to consider that for the given liquid flow velocity (U_L = 3.31 kg.m^{-2}s^{-1}), when the perforated Distributor-I is used for liquid distribution, it is necessary to increase the gas flow rate upto 0.1810 kg.m^{-2}s^{-1} (an increase of 13% approx than trickle flow) to obtain regular pulsing-foaming in the column. Figure 8 represents the influence of change in temperature on 60 ppm solution while coexistence of regime flow. Further increase in gas flow rate causes elevated pressure drop and varies upto 7,000-10,000 N/m (i.e. increment of about 12-18% approx). Here influence of high temperature is decisive factor to rapid increase in two phase pressure drop. This behavior is completely unpredictable and results varies with every new experiment.

   Both investigated systems at corresponding gas flow rate 0.2210 kg.m^{-2}s^{-1} are compared in Figure 9. These trends are surprise lie within maximum error ranges (also verify the dual natured flow) which ultimately yields into uneven conversion of products during regime transition changes. Figure 9 also shows the comparison with trendlines (during GCF to FPF transitional change) observed by different researchers [7,11,19], increasing pressures result into decrease in pulse variables whereas foaming pulses length varies significantly up and down over the height of column. Past researches introduced a pulse velocity correlation as a function of bed parameters packing size, and gas-liquid flow rates but neverwhere considered the effect of present issue of on overall reaction.
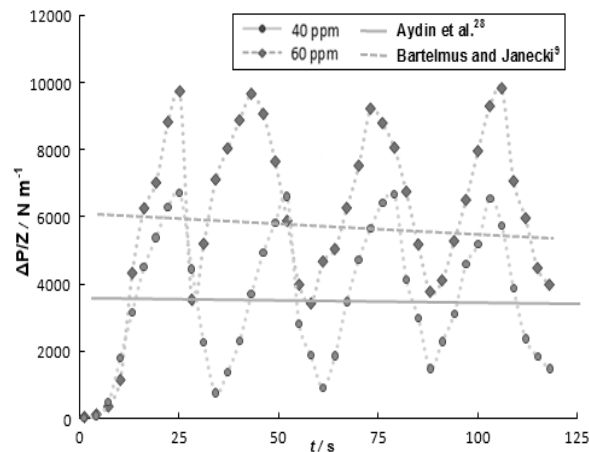

Fig. 9. Experimental two phase pressure drop (symbols) as a function of time and corresponding boundary (lines) for trickle to pulse flow conversion reported in literature. For 40 ppm (T = 28°C, U_G = 0.2210 kg.m^{-2}s^{-1} and U_L = 6.806 kg.m^{-2}s^{-1}) and 60 ppm air aqueous SLS systems (T = 28°C, U_G = 0.2210 kg.m^{-2}s^{-1} and U_L = 6.192 kg.m^{-2}s^{-1})

3.4. Variance

   In order to verify the coexistence of flow regimes persists, the evolution of local liquid satu-ration as a function of time at corresponding increasing temperature over 41 crossing points were estimated for dual natured flow corresponds to different gas and liquid velocities. A must followed step was to identify the presence of a high interaction unstable pulsing and foaming in the reactor, observed with voltage conductivity probe (Figure 10). Further, trends observed were plotted on the basis of average variation factor (standard deviation divided by the mean value of the successive measurements) shown in Figure 11.
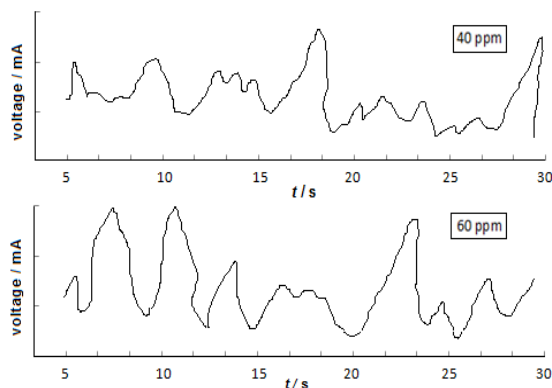

Fig. 10. Typical traces for present work flow irregularities recorded with voltage conductance probe. For 40 ppm solution, T = 60°C, U_G = 0.2210 kg.m^{-2}s^{-1} and U_L = 6.239 kg.m^{-2}s^{-1}; for 60 ppm solution, T = 60°C, U_G = 0.2210 kg.m^{-2}s^{-1} and U_L = 5.880 kg.m^{-2}s^{-1}
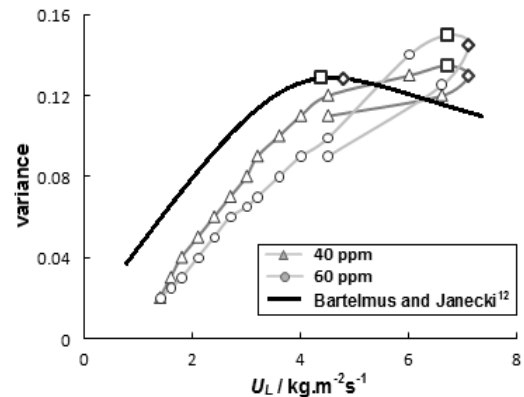
Fig. 11. Schematic illustration of coefficient of variation T as function of liquid flow velocity U_L, T = 60°C and U_G = 0.2210 kg.m^{-2}s^{-1}. Square vertex corresponds to regime transition between GCF to PF/FPF

The coefficient of variation T' evaluated from the variance and arithmetic average of fluctuating conductivity signals. The function T' compares the amplitude of voltage conductivity fluctuations with average signal value.

$$T' = \frac{\sqrt[4]{\overline{x^2}}}{X}$$

(2)

Where X is the mean average value, and x is the variance observed during occurrence of coexistence of flow regimes as a function of liquid flow rate u_L for constant gas flow. The maximum curve obtained is $(U_L, T') = (7, 0.15)$ corresponds higher pulse velocity found.

Trends show, the given variation factor data is a significant proof of coexistence of flow regimes. However it is reasonable to assume that, these variations may arise in high interaction pulse flow regime. Anyway, if the variation factor can specify the uneven pulsing/foaming existing in the reactor, plotting the dynamic liquid saturation trends at corresponding hydro-dynamic parameters is another prominent way of identifying a flow regime. Finally, to verify the present trends, the voltage spectrum of successive crossing points was observed to find out any pulse frequency exists which indicates the presence of uneven foaming pulsations at regular intervals in every experiment.

3.5. Effect of Temperature on Physiochemical Variables

As temperature increases, the dynamic viscosity of process liquid decreases due to weaken up of liquid shear stress at both liquid-solid and gas-liquid surface interfaces. This witnessed an uneven decreased amount of liquid held within bed in terms of Reynolds numbers (Figure 12) for both investigated systems of present study. The change of liquid surface tension with increasing temperature is expressed using liquid Reynolds numbers. The liquid viscosity provides gas penetration within liquid rivulets, causing foam bubble collapses on the solid surface. However, other than system gas-liquid influences, reductions in liquid viscosity and surface tension corresponds to system temperature are key responsible for less dynamic liquid holdup. Higher liquid throughput achieve an adequate dynamic holdup values for pulse formation to occur at elevated temperatures but dual nature of regime flow again play a significant role to decide the liquid hold up. Trends observed from Figure 12 also signifies the effect of destabilization of foam on liquid Reynolds numbers due to increasing temperatures.
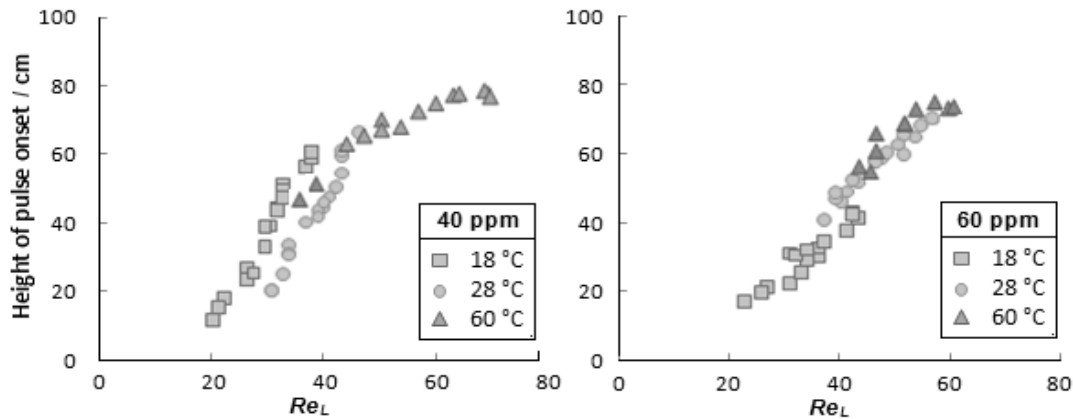

Fig. 12. Relative differences between column pulse onset height recorded as a function of liquid Reynolds numbers. For both air-aqueous 40 ppm and 60 ppm SLS systems corresponding $U_G = 0.2429$ kg.m^{-2}s^{-1} and 0.2770 kg.m^{-2}s^{-1} respectively.

None Boelhouwer [2,23] and Aydin [28-29] considered simultaneously augmenting system gas-liquid flow results into flow maldistribution during regime transition of trickle to pulse flow. There may be possibility of external forces and duration of reduced amplitude of pulsing in reactor, ultimately reducing energy transfer from trickle flow to pulsing foaming regime. This nature of fluid flow witnessed an improvement in rate of reaction through pulsing-foaming expansion but for small interval of time. Trends from present study observed travelling pulses in trickling flow regimes, whose pulse frequency were believed to be small to become turns into pulsing-foaming regime or least to improve mass transfer of process.

The behaviour of the foaming system during cyclic trickle bed operation (Figure 13) is inferred from the evolution coexistence of regimes(dual natured flow) at regular intervals of time. Figure 13 also shows, for foaming pulses rise to 30 cm height of catalyst bed, nearly completion of process flow cycle, little amount of gas bubbles left at accumulating liquid film. It is worthy of notice that the concentration of such gas bubbles is even not much prominent at catalyst bed height of 50 cm at lower liquid-gas velocities and vice versa. Foaming flow is activated over the 50 cm height of catalyst bed when the flow is switched to gas from liquid by the simultaneous large fluctuations in column pressure drop. For 60 ppm air-SLS system, foaming flow is much pronounced over bed height is 60-75 cm due to heavy accumulation of liquid allowed with cyclic operations. Further, when the flow is remained back to liquid only while gas is cut off, stagnant sub-millimeter bubbles remain in the bed even at increasing temperatures.
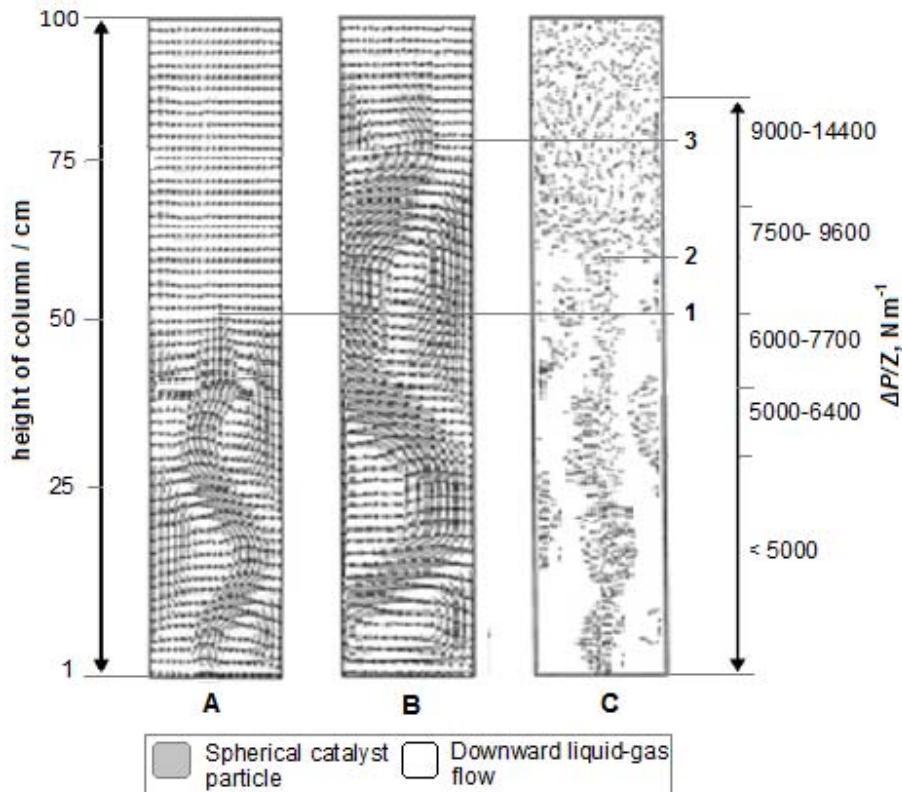

Fig. 13. Snapshot of relative deviations between experimental pulsing structure obtained as a function of time correspond to range of two phase pressure drop studied over height of packed column. For column A, view of GCF regime at t = 10 sec; column B, view of PF regime at t = 16 sec; column C, view of FPF regime at t = 25 sec; for corresponding air-aqueous 60 ppm system, T = 60° C, U_G = 0.2770 kg.m^{-2}s^{-1} and U_L = 3.880 kg.m^{-2}s^{-1}.

3.6. Gas-Liquid Distributor and Process Technique

Present trends revealed that, even with a good saturated liquid distribution over bed (using the perforated Distributor-A), two flow regimes can coexist in TBR operations. The foam formation ability of liquid decreases after each repeated periodic run and hence rise in dynamic liquid holdup values. While switch on the gas flow, an abrupt increase in pressure drop arise due to resistance facilitate by amount of liquid collected within bed portion.

Further, when using modified Distributor-B (Figure 14), regular pulsing and foaming during regime change were appeared without any increase in gas flow rate (when U_G = 0.1559 kg.m^{-2} s^{-1}) in every repeated experiment. Although a scientific explanation for these surprising trends is not still available but is worthy to remembered that, while using Distributor-A, 75% of column sectional were in high interaction foaming-pulsing regime corresponds to different gas-liquid flow rates. This time however, the high interaction pulsing-foaming zones were more to the

centred-front side of the catalyst bed column than to the centred-left region (as it was observed with Distributor A at corresponding low temperatures). This confirms the influence of both type of the liquid distributors used and the solid glass packing topology on the flow regimes.
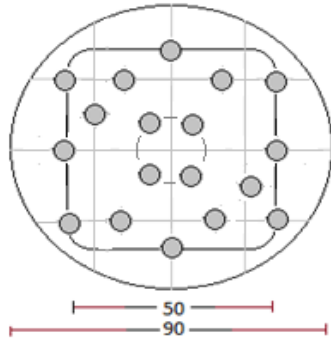

Fig. 14. Schematic of modified gas-liquid Distributor-B. Total number of holes: 18, diameter of each hole: 5mm
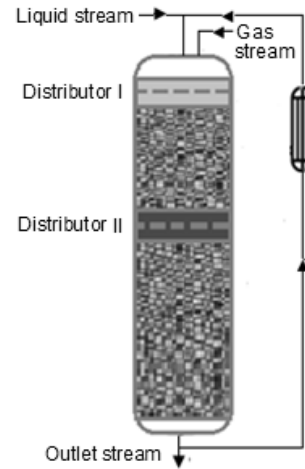
Figure 15. Technological scheme of TBR modified with two similar gas-liquid distributors.

   Trends observed from Distributor B shows a prominent reduce in maldistribution of flow but not completely (especially when working with high gas flow velocities more than 0.2059 kg.m^{-2}s^{-1}. An another attempt was made to nullify these kind of flow behaviour is use of two distributors in same column bed (Figure 15) which probably a new kind criterion in foamed TBR studies (none of information found in literature). This process significantly improve the maldistribution of flow in the form of coexistence of regimes. In this concern, four different distributor positions were investigated to detect most suitable one (Figure 16). It is clearly indicate from Figure 16 that, the liquid-gas Distributor-II situated at bed height of 60 cm is witness a prominent reduce in uneven pulsing-foaming and dual natured flow. Further, distributor II situated at 50 cm bed height also works significant but less prominent than 60cm height one.
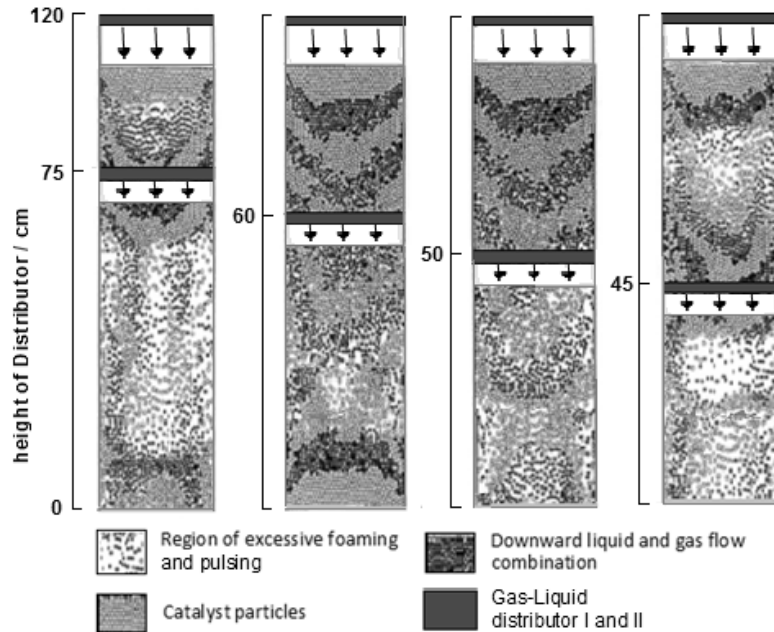

Fig. 16. Modified snapshot of relative deviation between flow behaviour (in FPF regime) formed over packed column equipped with two similar liquid distributors situated at four different heights. This reference is corresponds to air-aqueous 60 ppm system, T = 60° C, U_G = 0.2429 kg.m^{-2}s^{-1} and U_L = 5.120 kg.m^{-2}s^{-1}.

Present criterion also verified by two-phase pressure drop and dynamic liquid holdup trends observed (Figure 17 and 18). The high liquid shear stress interfaces within gas-liquid and liquid-solid contacts form interesting but gradual rise in pressure drops with increase in surfactant concentration (Figure 17). While comparing, 40 ppm and 60 ppm solution, shows a gradual elevation in two-phase pressure drop corresponds to liquid and gas flow velocities especially where coexistences of regimes arises. Figure 17 also shows, for both 40 ppm and 60 ppm air-SLS systems, an elevation in pressure drop is observed with increase in temperature as well as foam concentration during change of regime transition from GCF to PF/FPF. However, these trends show the two distributor technique seems more efficient as compared with using modified Distributor-A and B.
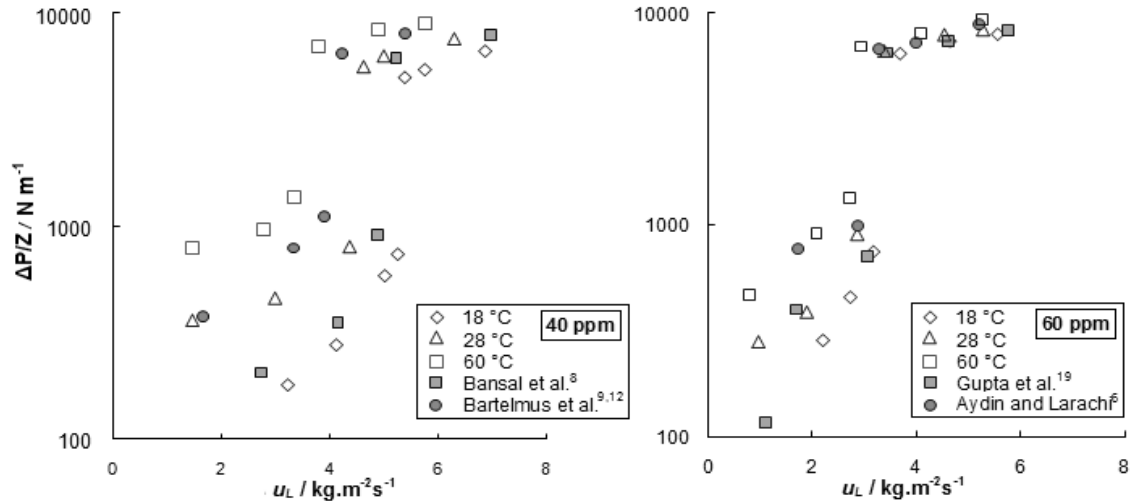

Fig. 17. Experimental two phase pressure drop as a function of liquid flow velocity and those were reported in literature. For air-aqueous 40 ppm and 60 ppm SLS systems at corresponding $U_G = 0.2429$ kg.m^{-2}s^{-1} and 0.2770 kg.m^{-2}s^{-1} respectively. Bansal et al.[8] corresponds to air-12 ppm SLS system; Bartelmus and Janecki [9,12] corresponds to air-glycerol system; Gupta et al.[19] corresponds to air-PEG system; Aydin and Larachi [6] corresponds to air-CTAB system
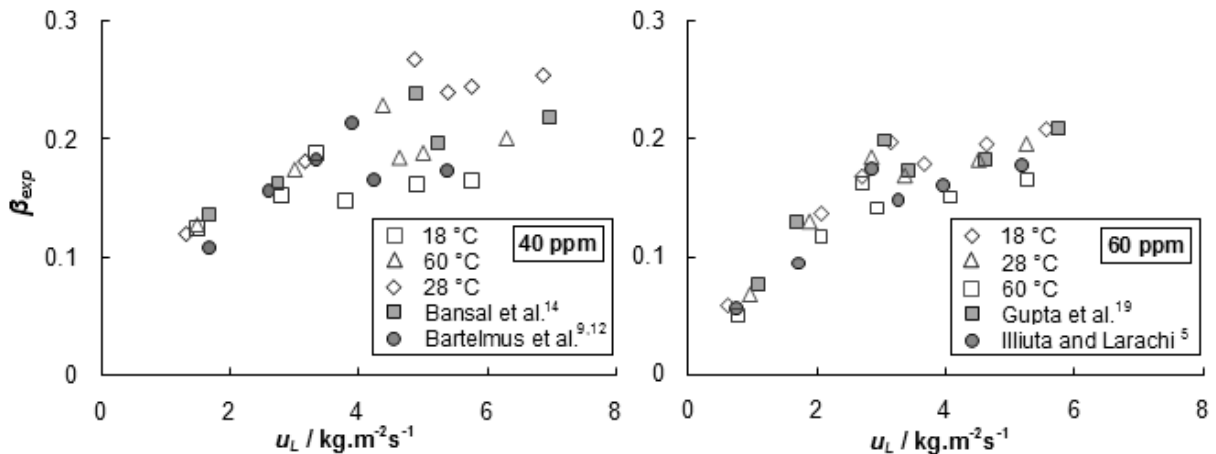

Fig. 18. Experimental dynamic liquid holdup as a function of liquid flow velocity and those were reported in literature. For air-aqueous 40 ppm and 60 ppm SLS system at corresponding $U_G = 0.2210$ kg.m^{-2}s^{-1}. Bansal et al.[14] corresponds to air-12 ppm SLS system; Bartelmus and Janeckim [9,12] corresponds to air-glycerol system; Gupta et al.[19] corresponds to air-PEG system; Illiuta and Larach [5] corresponds to air-CMC system.

Figure 18 confirmed that the interaction between gas and liquid phases are considerably small and barely affected by variations in the liquid flow rate. The effect of rise in system temperature evident a drastic decrease in dynamic liquid saturation values especially in PF/FPF regime. These results prove, the appearance of foam causes decrease in dynamic liquid saturation. Here noticeable thing is, earlier at same corresponding liquid and gas flow

rates, Distributor-A experiments showed an uneven zigzag dynamic liquid saturation response where coexistence of regimes appeared. These trends prominently revealed the importance of two distributor technique to improve these irregularities in foaming TBR.

4. Conclusions

The surface tension lowering corresponds to higher temperature would reduce the liquid carrying over expanding gas bubbles, result a higher contact angle between liquid and gas bubble surfaces. However, the mass transfer increases with elevated temperature. As a result, at higher temperatures, regime flow coexist near transition boundary. Here, the region for flow coexistence always seen during high concentrated 45 ppm and 60 ppm surfactants on air flow rate of more than 0.1012 $kg.m^{-2}s^{-1}$ during regime change from GCF to PF/FPF. Further, with negative fluctuation of 0.0055 $kg.m^{-2}s^{-1}$ air flow rate the unstable regime converts into trickle flow (GCF) and with positive fluctuation of 0.0055 $kg.m^{-2}s^{-1}$ air flow rate change unstable regime appears into pulsing foaming regime. Present study revealed a new flow regime of partially stable nature but has high significance in hydrodynamic studies of highly foaming liquids in trickle bed reactor.

The modified liquid Distributor-B lowered the possibilities of flow irregularities with compared to Distributor-A. While at corresponds to high liquid and gas flow velocities, modified Distributor-II also failed to nullify the flow maldistribution during regime transition change especially for high concentrations of air-SLS systems. However, means coexistence of flow distribution is not imaginary or limited to few physiochemical systems in TBR but possibly arises while working to high gas and liquid flow velocities. These results signify the importance of studying flow hydrodynamics near regime transition boundary and liquid distribution patterns involved the intimate relation between initial liquid distribution and flow regime in order to upgrade the performances of the trickle bed reactors. Indeed, it also allow studying the influence of liquid holdup and pressure drop variations occurred to improve performances of process.

A new technique of using two distributors (I and II) in TBR column significantly improve the results and yield efficiently, verified by dynamic liquid saturation and pressure drop trends observed. But it is difficult to work with this technique due to hydrodynamic irregularities which usually not arises during other (Distributor-A and B) TBR operations. This probably need a further study to get a better insight on liquid distribution patterns involved in foaming trickle bed methodology.

Acknowledgement

Abbreviations

TBR, trickle bed reactor; GCF, gas continuous flow; PF, pulsing flow; FPF, foaming pulsing flow; SLS, sodium lauryl sulphate; PEG, poly ethylene glycol; CMC, carboxymethylcellulose; CTAB, cetyltrimethylammoniumbromide

Notations

$$\Psi \qquad \left[\left(\frac{\rho_G}{\rho_{air}}\right)\left(\frac{\rho_L}{\rho_W}\right)\right]^{0.5} \left[\left(\frac{\sigma_W}{\sigma_L}\right)\left[\left(\frac{\mu_L}{\mu_W}\right)\left(\frac{\rho_W}{\rho_L}\right)^2\right]\right]^{0.33}$$

References

[1]   Tsochatzidis, N. A. Karabelas, A. J.:*Amer. Inst. Chem. Eng. J.* **41** (1995) 2371–2382.

[2]   Boelhouwer, J. G. Piepers, H. W. Drinkenburg, A. H.:*Chem. Eng. Sci.* **57** (2002) 4865-4876.

[3]   Larachi, F. Belfares, L. Grandjean, B. P. A.:*Int. Comm. Heat. Mass Trans*. **28** (2001) 595-600.

[4]   Burghardt, A. Bartelmus, G. Szlemp, A.: *Ind. Eng. Chem. Res.* 43 (2004) 4511–4521.

[5]   Iliuta, I. Larachi, F.:*Chem. Eng. Sci.* **59** (2004) 1199.

[6]   Aydin, B. Larachi, F.:*Chem. Eng. J.* **143** (2008) 236–243.

[7]   Sodhi, V. Gupta, R.: *Bull. Chem. React. Eng.* **6**:**2** (2011) 115-122.

[8]   Bansal, A. Wanchoo, R. K. Sharma, S. K.:*Chem. Eng. Comm.* **58** (2005) 111-118.

[9]   Bartelmus, G. Janecki, D.: *Chem. Eng. Process.* **42** (2003) 993–1005.

[10]   W. Lockhart, R. C. Martinelli, *Chem. Eng. Prog.* **45** (1949**)** 39–48.

[11]   Sodhi, V. Bansal, A.: *Int. J. Chem. Biol. Eng.* **4**:**1** (2011) 44-50.

[12]   Bartelmus, G. Janecki, D.: *Chem. Eng. Proc.* **43** (2004) 169–179.

[13]   Burghardt, A. Bartelmus, G. Janecki, D. Szlemp, A.:*Chem. Eng. Sci.* **57** (2002) 4855–4863.

[14]   Bansal, A. Wanchoo R. K. SSharma, . K.: *Ind. Eng. Chem.* **48**:**7** (2009) 3341-3350.

[15]   Ellman, M. J. Midoux, N. Laurent, A. Charpentier, J. C. :*Chem. Eng. Sci.* **43** (1998) 2201-2206.

[16]   Hasseni, W., Laurent, A.; Midoux, N.; Charpentier, J.C.:Régimes d'Écoulement dans un Réacteur Catalytique á Lit Fixe Arrosé Fonctionnant sous Pression à Co-courant de Gaz et de Liquide vers le Bas. Entropie. **1987**, 137, 127–133.

[17]   Larachi, F. Laurent, A. Midoux, J. Wild, G.:*Chem. Eng. Sci.* **46** (1991**)** 1233–1246.

[18]   Sai, P. S. T. Varma, Y. B. G.:*Amer. Inst. Chem. Eng. J.* **33** (1987) 2027–2035.

[19]   Gupta, R. Bansal, A. Sodhi, V.:Studies on dynamic liquid saturation in trickle bed reactor involving foaming liquids, International Conference on Advances in Chemical Engineering, (2009), Thapar University, Patiala, India, Feb 27-28, p. 410-413.

[20]   Haure, P. M. Hudgins, R. R. Silveston, P. L.: *Amer. Inst. Chem. Eng. J.* **35** (1989) 35, 1437-1444.

[21]   Lange, R. Hanika, J. Stradiotto, D. Hudgins, R. R. Silveston, P. L.:*Chem. Eng. Sci.* **49**:**24** (1992) 5615–5621.

[22]   Boelhouwer, J. G. Piepers, H. W. Drinkenburg, A. H.:*Chem. Eng. Sci.* **56** (2001) 1181-1187.

[23]   Boelhouwer, J. G. Piepers, H. W. Drinkenburg, A. H.:*Chem. Eng. Sci.* **54** (1989) 4661-4667.

[24]   Turco, F. Hudgins, R. R. Silveston, P. L. Sicardi, S. Manna, L. Banchero, M.:*Chem. Eng Sci.* **56** (2001) 1429-1434.

[25]   Wilke, C. R. Chang, P.:*Amer. Inst. Chem. Eng. J.* **1**:**2** (1955) 264–270.

[26]   Gianetto, A. Baldi, G. Specchia, V. Sicardi, S.:*Amer. Inst. Chem. Eng. J.* **24** (1976**)** 1087.

[27]   Attou, A. Ferschneider, G.:*Chem. Eng. Sci.* **55** (2000) 491–511.

[28]   Aydin, B. Fries, D. Lange, R. Larachi, F.:*Chem. Eng. Sci.* **62** (2007) 5554–5557.

[29]   Aydin, B. Hamidipour, M. Larachi, F.: *Chem. Eng Sci.* **62** (2007) 7539 – 7547.

[30]   Charpentier, J. C. Favier, M.: *Amer. Inst. Chem. Eng. J.* **21** (1975) 1213–1218.

[31]   Chou, T. S. Worley, F. L. Luss, D.: *Ind. Eng. Chem. Process Dev.* **16** (1997) 424.

[32]   Sodhi. V.: *Chem. Ind. Chem. Eng. Quart.* **18**:**3** (2012) 349-359.